PNAS
www.pnas.org

Supplementary Information for

Activity-dependent aberrations in gene expression and alternative splicing in a mouse model of Rett syndrome

Sivan Osenberg, Ariel Karten, Jialin Sun, Jin Li, Shaun Charkowick, Christy A. Felice, Mary Kritzer, Minh Vu Chuong Nguyen, Peng Yu, and Nurit Ballas

Corresponding authors:

Nurit Ballas
Email: nurit.ballas@stonybrook.edu

Peng Yu
Email: pengyu.bio@gmail.com

This PDF file includes:

Supplementary Materials and Methods
Figs. S1 and S2
References for SI
Other Supporting Information

Supplementary Materials and Methods

Animals

Mecp2-null mice (1) were obtained from the Jackson Laboratory (B6.129P2(C)-Mecp2tm1.1Bird/J) and maintained in a pure C57BL/6 background. WT and knockout *Mecp2* sequences were distinguished by PCR on tail biopsies using the following primers: Forward 5'- CCA TGC GAT AAG CTT GAT GA-3', forward 5'-GAC CCC TTG GGA CTG AAG TT-3', reverse 5'-CCA CCC TCC AGT TTG GTT TA-3'.

Kainic acid (KA) administration, seizure scoring, and dissection of the hippocampi

Kainic acid (SIGMA) was freshly prepared in a concentration of 1 mg/ml in 0.9% saline. WT and *Mecp2*-null male littermate mice were monitored for their overall health and behaviors, beginning at 4 weeks of age, using the previously described scoring system (2). At 7-weeks of age, a time when the *Mecp2*-null mice normally reach an average score of 5 for symptoms, both WT and *Mecp2*-null littermates were treated with KA by intra-peritoneal injection at a dosage of 23mg/kg body weight. Mice were monitored closely, and seizure stages were determined as previously described (3) and recorded. Untreated and kainic acid treated (40 and 68 minutes) mice were euthanized by rapid decapitation. Using RNAse-free instruments, the brains were immediately removed and placed in a shallow glass dish containing ice-cold HBSS solution. Brains were hemisected, and the alvear white matter sheath was used to guide blunt dissection of the left and right hippocampi. Tissues were flash frozen in liquid nitrogen, and then stored at -80 until used.

Primary cortical cultures and KCl treatment

Cortical neurons were isolated from P0-P1 WT and *Mecp2* knockout male littermate mice essentially as described (4). To enrich the cultures for neurons, the cells were plated on a poly-L-lysine-coated 6-well-dish at a density of 10^6 cells per well in Neurobasal-A medium supplemented with B27, 1 mM L-glutamine, and 100 U/mL penicillin/streptomycin (Invitrogene). After 48 hours, half of the medium was replaced with a fresh medium containing 2 μM Cytosine arabinoside (AraC) (SIGMA), and then half of the medium was replaced every other day with a fresh medium without AraC. To eliminate potential bias of cultural conditions, we proceeded with the experiment only when the WT and mutant cultures showed similar neuronal cell density and appeared healthy at 10-day-in vitro (DIV).

For neuron depolarization, 10 DIV WT and mutant cultures were treated with KCl for 3 h essentially as described (5) with the following modifications: Cultures were stimulated directly by adding 1 ml of KCl depolarization buffer [90 mM KCl, 2mM $CaCl_2$, 1 mM $MgCl_2$, and 10 mM 4-(2-hydroxyethyl)-1-piperazineethanesulfonic acid (HEPES)] to the cultures in a 1:2 dilution ratio. The final concentration of KCl in the neuronal medium was 35 mM (30 mM from the depolarization buffer plus 5 mM from the Neurobasal medium). For the KCl-untreated cultures, 1 ml of the same buffer without KCl was added in parallel. To further eliminate bias of cultural conditions, we induced neuron depolarization with KCl in two different wells for both, the WT and the mutant cultures, in each experiment.

Immunocytochemistry

Cells were fixed in PBS-buffered 4% paraformaldehyde for 15 minutes, washed with PBS three times, permeabilized with 0.1% Triton X-100 in PBS for 15 minutes, incubated in blocking buffer (2% BSA, 5% Donkey or Goat serum) for 1h at room temperature and then were incubated at 4 degree overnight with the following primary antibodies: Mouse anti-MAP2 (Millipore MAB3418)(1:200), rabbit anti-GFAP (Millipore AB5804)(1:1000), rabbit anti IBA-1 (WAKO 019-19741)(1:400), rat anti-MBP (Serotec MCA409S)(1:100), rabbit anti-MeCP2 (Cell Signaling 3456)(1:500), followed by incubation with the appropriate secondary antibodies conjugated to cyanine (Jackson ImmunoResearch Laboratories)(1:500) or Alexa Fluor (Invitrogen) (1:500). Images were collected on a Leica confocal laser-scanning (TCS-SP5) microscope.

RNA isolation, quantitative Real-time RT-PCR, and semi quantitative RT-PCR analyses

Total RNA was isolated using the miRNeasy Mini Kit (Qiagen). For reverse transcription, AMV-RT (New England BioLabs) was used. Quantitative Real-Time RT-PCR was performed in an ABI StepOnePlus real-time PCR system using SYBR-green PCR master mix (Applied Biosystems). For gene expression level analyses, the relative abundance of the specific mRNAs was normalized to *β-actin* mRNA. The relative abundance of alternative spliced variants was analyzed by semi quantitative RT-PCR or quantitative RT-PCR. For semi-quantitative RT-PCR, we used primers flanking the alternative exon/intron to amplify both inclusion and exclusion isoforms. The number of

PCR cycles chosen for each gene was within the PCR' exponential phase. For quantitative RT-PCR of alternative splicing, we used primer sets for 3 types of amplicons per each event: 1) 5' junction of the retention exon/intron, 2) 3' junction of the retention exon/intron, 3) exon/intron excision isoform. For the complete list of primers, see Dataset S16.

Total RNA library preparation and RNA-Sequencing

RNA sequencing (RNA-Seq) libraries were prepared using the KAPA Stranded RNA-Seq Kit with RiboErase (Kapabiosystems) in accordance with the manufacturer's instructions. Briefly, 500ng of total RNA were used for ribosomal depletion and fragmentation. Depleted RNA underwent first and second strand cDNA synthesis. cDNA was then adenylated, ligated to Illumina sequencing adapters, and amplified by PCR (using 9 cycles). Final libraries were evaluated using fluorescent-based assays including PicoGreen (Life Technologies) or Qubit Fluorometer (Invitrogen) and Fragment Analyzer (Advanced Analytics) or BioAnalyzer (Agilent 2100) and were sequenced to a depth of 60 million reads per sample on an Illumina HiSeq2500 sequencer (v4 chemistry) using 2 x 125-bp cycles.

Differential gene expression analysis using RNA-Seq data

Differential gene expression (DEG) analysis was performed as follows: The first 50 bp at the 5' end of the first read of each pair of the paired-end RNA-Seq data were aligned to the transcript sequences of the Gencode mouse basic annotation (release M12) (6) using STAR (2.5.3a) (7) with splicing alignment disabled and multiple alignments recorded.

The reads aligned to multiple gene symbols were discarded. Then, a count table was constructed by counting the number of reads that aligned to each gene symbol for each sample. To remove the batch effect for *in vitro* data, normalization and differential gene expression were performed using DESeq2 (8). As for the *in vivo* data, normalization and differential gene expression were performed using DESeq (9). FDR adjusted *q*-values were then calculated from the *p*-values in the tests using the Benjamini-Hochberg procedure (10). The log2-fold-changes of each comparison were also calculated for each gene. The differentially expressed genes were identified as $q < 0.05$.

Differential alternative splicing analysis using RNA-Seq data

Differential alternative splicing (DAS) analysis was performed as described (11). Specifically, the raw RNA-Seq reads were first aligned to mouse (mm9) genomes using STAR (version 2.5.1b) (7) with default settings. The uniquely mapped reads were retained to compute the number of reads for each exon and each exon-exon junction using the Python package HTSeq (12) with the UCSC KnownGene (mm9) annotation (13). The counts of the reads that were aligned to each isoform were modeled by the Dirichlet-multinomial (DMN) (14), and the significance of the changes in the alternative splicing events was tested using the likelihood ratio test (15). The adjusted *q*-values from the *p*-values in the likelihood ratio test were calculated using the Benjamini-Hochberg procedure (10). The differential alternative splicing events consist of seven splicing types, *i.e.* Exon skipping (ES), Alternative 5' splice sites (A5SS), Alternative 3' splice sites (A3SS), Mutually exclusive exons (ME), Intron retention (IR), Alternative first exons (AFE), and Alternative last exons (ALE). In addition, "percent spliced in" (PSI)

was applied to evaluate the percentage of the inclusion of variable exon relative to the total mature mRNA in the exon-skipping events (16). The PSI was expanded to determine the changes in splicing of all the seven splicing types in our DAS analysis. Particularly, the splicing event types ES, A5SS, A3SS, ME and IR include two isoforms, in which one isoform is longer. The PSI was calculated as the ratio of the expression of the longer isoform over the expression of both isoforms. For the splicing events of AFE and ALE, the PSI was calculated as the percentage of the usage of the proximal isoform (the isoform with the variable exon closer to the constitutive exon) relative to both isoforms of the event. The differential alternative splicing events are identified based on $|\Delta\text{PSI}| > 5\%$ and $q < 0.05$. For the precise location of exons in all RNAs that underwent alternative splicing, see Dataset S15.

Gene ontology analysis of the differentially expressed and the differentially alternative spliced genes

Gene ontology (GO) analysis was performed to examine the biological functions of the differentially expressed and the differential alternative spliced genes identified in the hippocampi of the kainic acid treated mice as described (17, 18). Specifically, Fisher's exact test was used to test the enrichment of genes in the GO terms over each defined gene set using the expressed genes as the background. To identify the robust biological relevant GO terms, the null hypothesis of Fisher's exact test was taken as H_0: log-odds-ratio < 2.0. The biological relevant GO terms were determined based on p-value < 0.05.

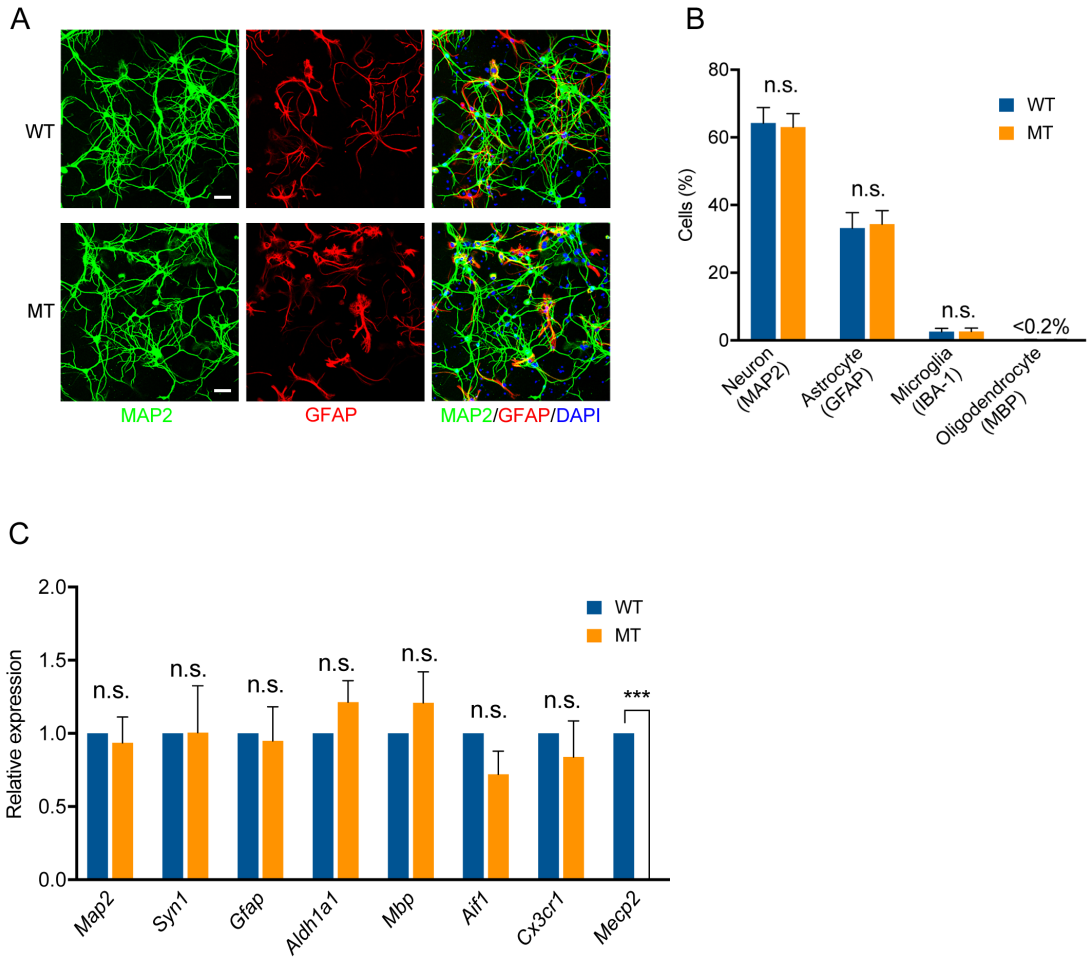

Fig. S1: WT and *Mecp2*-null cortical cultures at 10 DIV are enriched for neurons and comprise similar ratios of neurons:glia. **A)** Representative Images of immunostaining for neurons (MAP2) and astrocytes (GFAP) in WT and mutant (MT) cultures. Scale bars, 50 μm. **B)** The fractions of neurons (MAP2)/ astrocytes (GFAP)/ microglia (IBA-1)/ oligodendrocytes (MBP) are similar between the WT and mutant cultures. n=8 fields (694 cells) for WT culture, n=11 fields (842 cells) for mutant culture. Bar graphs display the mean percentage + SEM. Statistical significance was determined by unpaired 2-tailed student's *t*-test. n.s. not significant. **C)** Quantitative Real-time RT-PCR for cell-type-specific markers**.** Bar graphs showing that the markers for neurons

(*Map2*, *Syn1*), astrocytes (*Gfap*, *Aldh1a1*), microglia (*Aif1*/IBA-1, *Cx3cr1*), and oligodendrocytes (*Mbp*) are expressed to similar levels in WT and MT cultures. n=3 biological replicates used for the RNA-Seq analysis. In addition, quantification of *Mecp2* mRNA confirms its absence in the mutant cultures. Bar graphs display the mean relative RNA expression level + SEM. Statistical significance was determined by paired 2-tailed Student's *t*-test. n.s. not significant, ***$P < 0.001$.

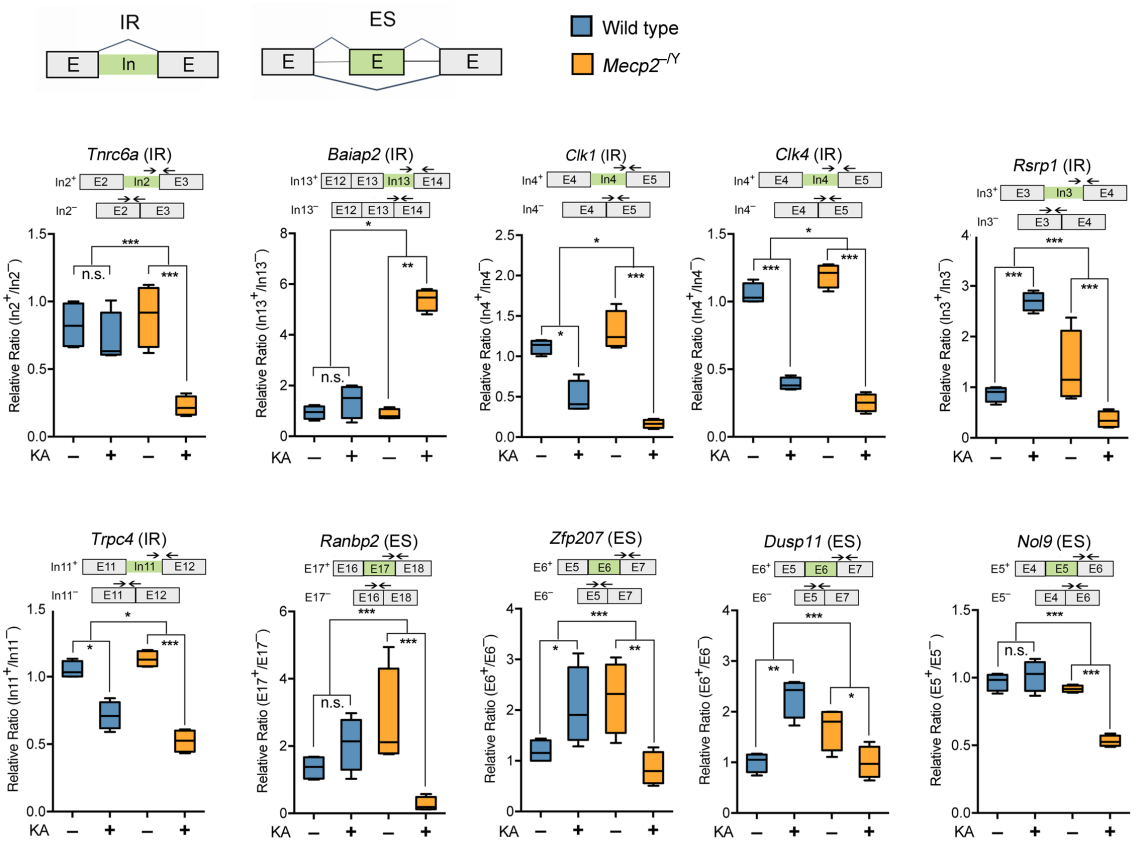

Fig. S2: Supportive validations for genes that underwent differential alternative splicing in the hippocampi of mutant mice when compared to WT mice upon KA treatment using 3'-junction primer sets. Top row shows diagrams of intron retention (IR), and exon skipping (ES). Boxplots show the relative ratio of retained *vs.* excised introns or included *vs.* excluded (skipped) exons in KA treated (+) and untreated (-) conditions. The diagram above each individual gene shows the two possible isoforms (included exon or intron in green or excised) with arrows indicating the location of the qPCR primers for the 3' junction of the inclusion isoform and the primers for the exclusion isoform. n= 4 biological replicates. Statistical significance for the qPCR analyses was determined by two-way ANOVA with multiple pairwise comparisons. **P*< 0.05, ***P*< 0.01, ****P*< 0.001.

References

1. Guy J, Hendrich B, Holmes M, Martin JE, & Bird A (2001) A mouse Mecp2-null mutation causes neurological symptoms that mimic Rett syndrome. *Nat Genet* 27(3):322-326.
2. Nguyen MV*, et al.* (2012) MeCP2 Is Critical for Maintaining Mature Neuronal Networks and Global Brain Anatomy during Late Stages of Postnatal Brain Development and in the Mature Adult Brain. *The Journal of neuroscience : the official journal of the Society for Neuroscience* 32(29):10021-10034.
3. Wu G*, et al.* (2005) Enhanced susceptibility to kainate-induced seizures, neuronal apoptosis, and death in mice lacking gangliotetraose gangliosides: protection with LIGA 20, a membrane-permeant analog of GM1. *The Journal of neuroscience : the official journal of the Society for Neuroscience* 25(47):11014-11022.
4. Ballas N, Lioy DT, Grunseich C, & Mandel G (2009) Non-cell autonomous influence of MeCP2-deficient glia on neuronal dendritic morphology. *Nature neuroscience* 12(3):311-317.
5. Ataman B*, et al.* (2016) Evolution of Osteocrin as an activity-regulated factor in the primate brain. *Nature* 539(7628):242-247.
6. Harrow J*, et al.* (2006) GENCODE: producing a reference annotation for ENCODE. *Genome biology* 7 Suppl 1:S4 1-9.
7. Dobin A*, et al.* (2013) STAR: ultrafast universal RNA-seq aligner. *Bioinformatics* 29(1):15-21.
8. Love MI, Huber W, & Anders S (2014) Moderated estimation of fold change and dispersion for RNA-seq data with DESeq2. *Genome biology* 15(12):550.
9. Anders S & Huber W (2010) Differential expression analysis for sequence count data. *Genome biology* 11(10):R106.
10. Benjamini Y & Hochberg Y (1995) Controlling the False Discovery Rate: A Practical and Powerful Approach to Multiple Testing. *J. R. Statist. Soc. B* 57:289-300.
11. Li J & Yu P (2018) Genome-wide transcriptome analysis identifies alternative splicing regulatory network and key splicing factors in mouse and human psoriasis. *Sci Rep* 8(1):4124.
12. Anders S, Pyl PT, & Huber W (2015) HTSeq--a Python framework to work with high-throughput sequencing data. *Bioinformatics* 31(2):166-169.
13. Hsu F*, et al.* (2006) The UCSC Known Genes. *Bioinformatics* 22(9):1036-1046.
14. Yu P & Shaw CA (2014) An efficient algorithm for accurate computation of the Dirichlet-multinomial log-likelihood function. *Bioinformatics* 30(11):1547-1554.
15. Casella G & Berger RL (2001) *Statistical Inference* Second Edition Ed.
16. Katz Y, Wang ET, Airoldi EM, & Burge CB (2010) Analysis and design of RNA sequencing experiments for identifying isoform regulation. *Nature methods* 7(12):1009-1015.
17. Ashburner M*, et al.* (2000) Gene ontology: tool for the unification of biology. The Gene Ontology Consortium. *Nat Genet* 25(1):25-29.
18. Guo Z*, et al.* (2016) Possible mechanisms of host resistance to Haemonchus contortus infection in sheep breeds native to the Canary Islands. *Sci Rep* 6:26200.

Other Supporting Information Files

Datasets S1-S16.

Differential gene expression and alternative splicing between WT and *Mecp2*-null mice at steady state and upon neuronal activity.

Datasets S1-S3: RNA-Seq analysis of gene expression performed on untreated or KCl-treated, WT and mutant neuron-enriched cortical cultures, at 10 days in vitro.

Datasets S4-S14: RNA-Seq analyses performed on hippocampi of 7-week-old, WT and mutant male littermate mice, either untreated or treated with Kainic acid for 40 min or 68 min: Datasets S4-S8, gene expression analysis; Datasets S9-S14, alternative splicing analysis.

Dataset S15: Exon locations in the genes that underwent alternative splicing.

Dataset S16: Sequences of the primer sets used for quantitative and semi-quantitative RT-PCR.